Atmospheric
Chemistry
and Physics
Discussions

1

Trend of atmospheric mercury concentrations at Cape Point for 1995 – 2004 and since 2007

Lynwill G Martin[1], Casper Labuschagne[1], Ernst-Günther Brunke[1], Andreas Weigelt[2*], Ralf Ebinghaus[2], Franz Slemr[3]

[1]South African Weather Service c/o CSIR, P.O.Box 320, Stellenbosch 7599, South Africa

[2]Helmholtz-Zentrum Geesthacht (HZG), Institute of Coastal Research, Max-Planck-Strasse 1, D-21502 Geesthacht, Germany,

[3]Max-Planck-Institute for Chemistry, Hahn-Meitner-Weg 1, D-55128 Mainz, Germany

*now at: Federal Maritime and Hydrographic Agency (BSH), Hamburg, Germany

Lynwill Martin: lynwill.martin@weathersa.co.za

Casper Labuschagne: casper.labuschagne@weathersa.co.za

Ernst-Günther Brunke: egbrunke@gmail.com

Andreas Weigelt: andreas.weigelt@bsh.de

Ralf Ebinghaus: ralf.ebinghaus@hzg.de

Franz Slemr: franz.slemr@mpic.de

Atmospheric
Chemistry
and Physics
Discussions

2

Abstract

27 Long-term measurements of gaseous elemental mercury (GEM) concentrations at
28 Cape Point, South Africa, reveal a downward trend between September 1995 and
29 December 2005 and an upward one since March 2007 until June 2015 implying a
30 change in trend sign between 2004 and 2007. The trend change is qualitatively
31 consistent with the trend changes in GEM concentrations observed at Mace Head,
32 Ireland, and in mercury wet deposition over North America suggesting a change in
33 worldwide mercury emissions.
34 Seasonally resolved trends suggest a modulation of the overall trend by regional
35 processes. The trends in absolute terms (downward in 1995 – 2004 and upward in
36 2007 – 2015) are the highest in austral spring (SON) coinciding with the peak in
37 emissions from biomass burning in South America and southern Africa. The influence
38 of trends in biomass burning is further supported by a biennial variation in GEM
39 concentration found here and an ENSO signature in GEM concentrations reported
40 recently.

Introduction

44 Mercury and especially methyl mercury which bio-accumulates in the aquatic
45 nutritional chain are harmful to humans and animals (e.g. Mergler et al., 2007;
46 Scheuhammer et al., 2007; Selin, 2009; and references therein). Mercury, released
47 into the environment by natural processes and by anthropogenic activities, cycles
48 between the atmosphere, water, and land reservoirs (Selin et al., 2008). In the
49 atmosphere, mercury occurs mostly as gaseous elemental mercury (GEM) which with
50 an atmospheric lifetime of 0.5 – 1 yr can be transported over large distances (Lindberg
51 et al., 2007). Mercury is thus a pollutant of global importance and as such on the
52 priority list of several international agreements and conventions dealing with
53 environmental protection and human health, including the United Nations
54 Environment Program (UNEP) Minamata convention on mercury
55 (www.mercuryconvention.org).

57 Because of fast mixing processes in the atmosphere, monitoring of tropospheric
58 mercury concentrations and of its deposition will thus be the most straightforward

Atmospheric
Chemistry
and Physics
Discussions

3

59   way to verify the decrease of mercury emissions expected from the implementation of

60   the Minamata convention. Regular monitoring of atmospheric mercury started in the

61   mid-1990s with the establishment of mercury monitoring networks in North America

62   (Temme et al., 2007; Prestbo and Gay, 2009; Gay et al., 2013). Until 2010 only a few

63   long-term mercury observations have been reported from other regions of the northern

64   hemisphere and hardly any from the southern hemisphere (Sprovieri et al., 2010). The

65   Global Mercury Observation System (GMOS, www.gmos.eu) was established in 2010

66   to extend the mercury monitoring network, especially in the southern hemisphere

67   (Sprovieri et al., 2016).

68

69   Decreasing atmospheric mercury concentrations and wet mercury deposition have

70   been reported for most sites in the northern hemisphere (Temme et al., 2007; Prestbo

71   and Gay, 2009; Ebinghaus et al., 2011; Gay et al., 2013). At Cape Point, the only site

72   in the southern hemisphere with a long-term record exceeding a decade, decreasing

73   mercury concentrations were also observed between 1996 and 2004 (Slemr et al.,

74   2008). The worldwide decreasing trend has been at odds with increasing mercury

75   emissions in most inventories (Muntean et al., 2014, and references therein).

76   Soerensen et al. (2012) thought that decreasing mercury concentrations in sea water of

77   the North Atlantic were responsible for the decrease, at least in the northern

78   hemisphere. The most recent inventories, however, attribute the decrease of

79   atmospheric mercury concentrations to a decrease in mercury emissions since 1990

80   (Zhang et al., 2016). The decrease in mercury emissions was attributed to the decrease

81   of emissions from commercial products, changing speciation of emission from coal-

82   fired power plants, and to the improved estimate of mercury emissions from artisanal

83   mining. According to Zhang et al. (2016) the worldwide anthropogenic emissions

84   decreased from 2890 Mg yr^{-1} in 1990 to 2160 Mg yr^{-1} in 2000 and increased slightly

85   to 2280 Mg yr^{-1} in 2010.

86

87   In the first approximation, the observed trends in atmospheric mercury should follow

88   these changes. There is indeed some recent evidence that the downward trend in the

89   northern hemisphere is slowing or even turning upwards (Weigelt et al., 2015; Weiss-

90   Penzias et al., 2016). Here we report and analyse the trends of atmospheric mercury

91   concentrations at the GAW station Cape Point between 1995 and 2004 and since

92   March 2007 until June 2015.

Atmospheric
Chemistry
and Physics
Discussions

4

93 **Experimental**

94

95   The Cape Point site (CPT, 34° 21′S, 18° 29′E) is operated as one of the Global

96   Atmospheric Watch (GAW) baseline monitoring observatories of the World

97   Meteorological Organization (WMO). The station is located on the southern tip of the

98   Cape Peninsula within the Cape Point National Park on top of a peak 230 m above sea

99   level and about 60 km south from Cape Town. The station has been in operation since

100   the end of the 1970s and its current continuous measurement portfolio includes Hg,

101   CO, O_3, CH_4, N_2O, ^{222}Rn, CO_2, several halocarbons, particles, and meteorological

102   parameters. The station receives clean marine air masses for most of the time.

103   Occasional events with continental and polluted air can easily be filtered out using a

104   combination of CO and ^{222}Rn measurements (Brunke et al., 2004). Based on the ^{222}Rn

105   ≤ 250 mBq m^{-3} criterion about 35% of the data are classified annually as baseline.

106

107   Gaseous elemental mercury (GEM) was measured by a manual amalgamation

108   technique (Slemr et al., 2008) between September 1995 and December 2004 and by

109   the automated Tekran 2537B instrument (Tekran Inc., Toronto, Canada) since March

110   2007. Typically, ~ 13 measurements per month were made using the manual

111   technique, each covering 3 h sampling time. The manual technique was compared

112   with the Tekran technique in an international intercomparison (Ebinghaus et al., 1999)

113   and provided comparable results.

114

115   Since March 2007 GEM was measured using an automated dual channel, single

116   amalgamation, cold vapor atomic fluorescence analyzer (Tekran-Analyzer Model

117   2537 A or B, Tekran Inc., Toronto, Canada). The instrument utilized two gold

118   cartridges. While one is adsorbing mercury during a sampling period, the other is

119   being thermally desorbed using argon as a carrier gas. Mercury is detected using cold

120   vapor atomic fluorescence spectroscopy (CVAFS). The functions of the cartridges are

121   then interchanged, allowing continuous sampling of the incoming air stream.

122   Operation and calibration of the instruments follow established and standardized

123   procedures of the GMOS (Global Mercury Observation System, www.gmos.eu)

124   project. The instrument was run with 15 min sampling frequency while 30 min

125   averages were used for the data analysis. All mercury concentrations reported here are

126   given in ng m^{-3} at 273.14 K and 1013 hPa.

Atmospheric
Chemistry
and Physics
Discussions

Open Access

EGU

127   The Mann-Kendal test for trend detection and an estimate of Sen´s slope were made

128   using the program by Salmi et al. (2002).

129

130   **Results**

131

132   1. Trend

133

134   The upper panel of Figure 1 shows monthly average GEM concentrations calculated

135   from all data since March 2007 until June 2015 and in the lower panel monthly

136   average GEM concentrations were calculated from baseline data, i.e. GEM

137   concentrations measured at ^{222}Rn concentration $\leq$ 250 mBq m^{-3}. The slope of the least

138   square fit of all data (0.0222 $\pm$ 0.0032 ng m^{-3} yr^{-1}, n=99) is not significantly different

139   from the slope calculated from the baseline data only (0.0219 $\pm$ 0.0032 ng m^{-3} yr^{-1}).

140   Sen´s slope and trend significance for all (0.0210 ng m^{-3} yr^{-1}) and baseline (0.0208 ng

141   m^{-3} yr^{-1}) data are listed in Table 1. Sen´s slopes tend to be somewhat lower than the

142   slopes from the least square fits but they are in agreement within their 95%

143   uncertainty range. All trends are highly significant, i.e. at level $\geq$ 99.9%. The results

144   are essentially the same whether monthly median or monthly average concentrations

145   are used. This shows that the trend is robust and not influenced by occasional

146   pollution or depletion events.

147

148   The trends were calculated for different seasons (austral fall - March, April, May;

149   winter – June, July, August; spring – September, October, November; and summer –

150   December, January, February) for the period since March 2007 until June 2015 from

151   all and baseline data. These are listed in Table 1. Although the 95% uncertainty

152   ranges of seasonal Sen´s slopes overlap, the least square fit slopes for different

153   seasons are statistically different at > 99% significance level. Irrespective of whether

154   monthly averages or medians or least square fit or Sen´s slope are used, a consistent

155   picture emerges with upward trends where the slopes decrease in the following order:

156   austral spring (SON) > summer (DJF) > winter (JJA) > fall (MAM).

157

158   For comparison we also calculated the trends for the manually measured GEM

159   concentrations during the period September 1995 – December 2004 periods. Baseline

160   data were not filtered out from this data set because a) on average only 13

Atmospheric
Chemistry
and Physics
Discussions

Open Access

EGU

6

161 measurements were available per month and b) ^{222}Rn was measured only since March

162 1999 and cannot thus be used as criterion for the whole period. In Table 2 we list the

163 trends calculated from the least square fit of the monthly medians. Monthly averages

164 provide qualitatively the same trends with lower significance, because of their larger

165 sensitivity to extreme GEM concentrations. The trend of all monthly medians of -

166 0.0176 ± 0.0027 ng m^{-3} year^{-1} is somewhat higher than -0.015 ± 0.003 ng m^{-3} year^{-1}

167 (Slemr et al., 2008) calculated from the 1996 and 1999 – 2004 annual averages but

168 within the uncertainty of both calculations.

169

170 Seasonal trends for the 1995 – 2004 period are all downward and their slopes are

171 decreasing in the following order: austral fall > summer > winter > spring (note the

172 negative sign of the slopes). The difference between fall and summer as well as

173 between winter and spring is not significant. In absolute terms the slope during austral

174 autumn (MAM) is the smallest and for spring (SON) is the highest for both the 1995 –

175 2004 and 2007 – 2015 data sets.

176

177   2. Seasonal variation

178

179 For analysis of seasonal variation we detrended the monthly averages using their least

180 square fits. The detrended monthly averages were then averaged according to months.

181 Figure 2a shows the seasonal variation of relative monthly averages with their

182 respective standard error. No systematical seasonal variation is apparent in this plot.

183 We noted, however, a two-year periodicity in the monthly averages. Figure 2b shows

184 the monthly averages of the detrended monthly values for a 2year period. Despite the

185 somewhat higher standard errors of the monthly averages (number of averaged

186 months for biennial variation being only half of those for the seasonal variation), the

187 monthly averages vary between 0.95 and 1.05 as do the monthly averages for the

188 seasonal variation (Figure 1a). Taken collectively, however, the relative GEM

189 concentrations during the second year are significantly (>99.9%) higher than those in

190 the first year. This is a clear sign of a biennial variation of GEM concentrations at

191 Cape Point.

192

193 **Discussion**

194

Atmospheric
Chemistry
and Physics
Discussions

195   Tropospheric biennial oscillations (TBO) in tropospheric temperature, pressure, wind

196   field, monsoon, etc. has been previously reported in the literature (e.g. Meehl, 1997,

197   Meehl and Arblaster, 2001, 2002, Zheng and Liang, 2005). Meehl and Arblaster

198   (2001) also report that TBO with roughly a $2 - 3$ years period encompasses most

199   ENSO years with their well-known biennial tendency. Slemr et al. (2016) analysed

200   mercury data from Cape Point in South Africa, Mace Head in Ireland, and from

201   CARIBIC measurements in the upper troposphere and found an ENSO signature in all

202   these data sets. Thus the finding of biennial variation of GEM concentrations at Cape

203   Point is consistent with the ENSO influence.

204

205   All GEM concentrations show an upward trend of 0.0210 (0.0127 – 0.0284) ng m^{-3}

206   year^{-1} between March 2007 and June 2015. This trend is almost identical with 0.0208

207   (0.0141 – 0.0280) ng m^{-3} year^{-1} when only baseline (i.e. GEM concentrations at ^{222}Rn

208   concentrations ≤ 250 mBq m^{-3}) are considered. Occasional pollution and depletion

209   events (Brunke et al., 2010; 2012) thus do not influence the trend of the all data set. A

210   decreasing trend of - 0.015 ± 0.003 ng m^{-3} yr^{-1} was derived from annual medians of all

211   GEM concentrations at Cape Point measured manually during the years 1996 and

212   1999 – 2004 (Slemr et al., 2008). These data were obtained by a manual technique

213   and have an annual coverage of only about 300 hours per year, i.e. about 3% in

214   contrast to the Tekran measurements since 2007 where the coverage was nearly

215   100%. Here we derive a downward trend of -0.0176 ± 0.0027 ng m^{-3} year^{-1} from the

216   least square fit of the monthly medians since September 1995 until December 2004.

217   Despite the different temporal coverage (because of incomplete data set, only the

218   1996 and 1999 – 2004 annual medians were used by Slemr et al. (2008)), both trends

219   are in good agreement. Because of the small data coverage and ^{222}Rn data available

220   only since 1999 we were not able to filter out the baseline data for the whole 1995 –

221   2004 period and to determine their trend separately.

222

223   The upward trend after March 2007 and the downward trend between 1995 and 2004

224   were measured by different techniques: the former one with a Tekran instrument and

225   the latter one using the manual technique. For reasons outside of our control we could

226   not operate both techniques side by side for a reasonable length of time. Although the

227   measurements by both techniques agreed well during an international field

228   intercomparison (Ebinghaus et al., 1999), we do not claim here that they are

Atmospheric
Chemistry
and Physics
Discussions

8

229   comparable without an intercomparison of both techniques at Cape Point. Assuming

230   internal consistency of each of the data sets, it is however obvious that the decreasing

231   trend between 1995 and 2004 turned to an increasing one since 2007 implying that the

232   turning point was located between 2004 and 2007.

233

234   The changing trend at Cape Point is not the only sign that the hemispheric trends in

235   mercury concentrations are changing. An analysis of 1996 – 2013 data from Mace

236   Head, classified according to the geographical origin of the air masses, showed a) that

237   the downward trend of mercury concentration in air masses originating from over the

238   Atlantic Ocean south of 28°N is substantially lower than for all other classes

239   originating north of 28°N and b) that all downward trends for air masses originating

240   from north of 28°N are decelerating (Weigelt et al., 2015). The apparent inconsistency

241   that no decelerating trend for air masses from south of 28°N was found can be

242   explained by the fact that the changes of a smaller trend are likely to be more difficult

243   to detect. Weiss-Penzias et al. (2016) recently reported that the wet mercury

244   deposition was decreasing at 53% of the sites in the U.S. and Canada and was

245   increasing at none of the sites over the period 1997 – 2013. Over the period 2008-

246   2013, however, the mercury wet deposition was decreasing only at 6% of the sites but

247   was increasing at 30% of the sites. Thus the sign change of the trend at Cape Point

248   somewhere between 2004 and 2007 is just one more indication that trends in

249   atmospheric mercury concentrations are changing world-wide. The most recent

250   inventory by Zhang et al. (2016) estimated that the worldwide anthropogenic

251   emissions decreased from 2890 Mg yr^{-1} in 1990 to 2160 Mg yr^{-1} in 2000 and

252   increased slightly to 2280 Mg yr^{-1} in 2010.

253

254   Seasonally resolved trends may provide some information about the processes

255   influencing the trends at Cape Point. For the period 1995 - 2005 we find the smallest

256   downward trend (-0.0132 ng m^{-3} $year^{-1}$) in austral fall (MAM) and the largest one (-

257   0.0198 ng m^{-3} $year^{-1}$) in austral spring (SON). In the 2007 – 2015 data the lowest

258   upward trend is found for austral fall (MAM, around 0.010 ng m^{-3} $year^{-1}$) and the

259   highest in austral spring (SON, ~ 0.037 ng m^{-3} $year^{-1}$). The difference in seasonal

260   GEM trends may originate from the seasonal trends of GEM emissions or from

261   climatological shifts in regional transport patterns or both.

262

9

263   Hg emissions from coal fired power plants, the largest anthropogenic Hg source, tend

264   to be nearly constant over the year (Rotty, 1997). On the contrary, biomass burning is

265   a highly seasonal phenomenon with maximum emissions during August - September

266   both in southern America and southern Africa (Duncan et al., 2003; van der Werff et

267   al., 2006). Taking into account a delay by ~ 3 months due to intrahemispherical air

268   mixing time,he October - November coincide with the maximum seasonal trends: an

269   upward one for 2007 – 2015 and a downward one for the 1995 – 2004 periods.

270   Biomass burning emission inventories suggest a small decrease in CO emissions from

271   Africa and more pronounced one from South America between 1997 and 2004, but

272   differences between different inventories render it very uncertain (Granier et al.,

273   2011). As the emission estimates by Granier et al. (2011) end in 2010, no trend in

274   emissions from biomass burning in 2007 – 2015 period can be given. Nonetheless, the

275   ambient Cape Point CO data has shown a measurable decrease during 2003 till 2014

276   (Toihir et al., 2015). We tried to calculate seasonal trends of baseline CO mixing

277   ratios for 1995 – 2004 and 2007 – June 2015 periods but none of the trends was

278   significant. The 1995 – 2004 and 2007 – June 2015 periods are probably too short to

279   reveal trends in CO data obscured by strong seasonal and interannual variations.

280   Nevertheless, the ENSO signature both in Hg and CO data from Cape Point, Mace

281   Head, and CARIBIC was found to be consistent, within large uncertainty margins,

282   with emissions from biomass burning (Slemr et al., 2016). In summary, seasonal

283   variations of emissions from biomass burning in southern Africa and America as well

284   as ENSO signature are consistent with a hypothesis of emissions from biomass

285   burning as a major driving force behind the different seasonal trends as seen in the

286   Cape Point data.

287

288   **Conclusions**

289

290   We report here an increasing trend for mercury concentrations at Cape Point for the

291   period 2007 – 2015. As mercury concentrations at Cape Point decreased over the

292   period 1996 – 2004 we conclude that the trend must have changed sign between 2004

293   and 2007. Such a change is qualitatively consistent with the trend changes observed in

294   atmospheric mercury concentrations at Mace Head in the Northern Hemisphere

295   (Weigelt et al., 2015) and in mercury wet deposition at sites in North America (Weiss-

296   Penzias et al., 2016). Combining all this evidence it seems that the worldwide

Atmospheric
Chemistry
and Physics
Discussions

Open Access

EGU

297 mercury emissions are now increasing, after a decade or two of decreasing emissions.

298 This finding is consistent with the temporal development of mercury emissions in the

299 most recent mercury inventory (Zhang et al., 2016).

300

301 For both periods, 1995 – 2004 and 2007 – 2015, seasonally resolved trends were

302 different in different seasons. We believe that the observed trends of GEM

303 concentrations at Cape Point result from the trend of worldwide mercury emissions

304 and are additionally modulated by regional influences. During 1995 – 2004 the

305 highest downward trend was observed in austral spring (SON) and winter (JJA). For

306 the 2007 – 2015 period the highest upward trend was found in austral spring. Hg

307 emissions from biomass burning in South America and southern Africa both peak in

308 August and September (Duncan et al., 2003, van der Werff et al., 2006). Although the

309 trend of these emissions is uncertain because of differences between different

310 emission inventories (Granier et al., 2013), it can produce different trends in different

311 seasons. Biennial variation of the GEM concentrations at Cape Point, reported here,

312 suggest that climatological changes of transport patterns can also play a role in

313 seasonally different trends. The detection of the ENSO signature in GEM

314 concentrations at Cape Point (Slemr et al., 2016) is consistent with the influence of

315 both emissions from biomass burning and changing regional transport patterns.

316

Acknowledgment

324

325 **References**

326

327 Brunke, E.-G., Labuschagne, C., Parker, B., Scheel, H.E., Whittlestone, S.: Baseline

328 air mass selection at Cape Point, South Africa: Application of ^{222}Rn and other filter

329 criteria to CO_2, Atmos. Environ. 38, 5693-5702, 2004.

330

11

331   Brunke, E.-G., Kabuschagne, C., Ebinghaus, R., Kock, H.H., and Slemr, F.: Gaseous

332   elemental mercury depletion events observed at Cape Point during 2007 – 2008,

333   Atmos. Chem. Phys., 10, 1121-1131, 2010.

334

335   Brunke, E.-G., Ebinghaus, R., Kock, H.H., Labuschagne, C., Slemr, F.: Emissions of

336   mercury in southern Africa derived from long-term observations at Cape Point, South

337   Africa, Atmos. Chem. Phys. 12, 7465-7474, 2012.

338

339   Duncan, B.N., Martin, R.V., Staudt, A.C., Yevich, R., and Logan, J.A.: Interannual

340   and seasonal variability of biomass burning emissions constrained by satellite

341   observations, J. Geophys. Res., 108; D2, 4100, doi:10.1029/2002JD002378, 2003.

342

343   Ebinghaus, R., Jennings, S.G., Schroeder, W.H., Berg, T., Donaghy, T., Guentzel, J.,

344   Kenny, C., Kock, H.H., Kvietkus, K., Landing, W., Mühleck, T., Munthe, J., Prestbo,

345   E.M., Schneeberger, D., Slemr, F., Sommar, J., Urba, A., Wallschläger, D., Xiao, Z.:

346   International field intercomparison measurements of atmospheric mercury species,

347   Atmos. Environ. 33, 3063-3073, 1999.

348

349   Ebinghaus, R., Jennings, S.G., Kock, H.H., Derwent, R.G., Manning, A.J., and Spain,

350   T.G.: Decreasing trend in total gaseous mercury observations in baseline air at Mace

351   Head, Ireland, from 1996 to 2009, Atmos. Environ. 45, 3475-3480, 2011.

352

353   Gay, D.A., Schmeltz, D., Prestbo, E., Olson, M., Sharac, T., and Tordon, R.: The

354   Atmospheric Mercury Network: measurement and initial examination of an ongoing

355   atmospheric mercury record across North America, Atmos. Chem. Phys., 13, 11339-

356   11349, 2013.

357

358   Granier, C., Bessagnet, B., Bond, T., D´Angiola, A., Denier van der Gon, H., Frost,

359   G.J., Heil, A., Kaiser, J.W., Kinne, S., Klimont, Z., Kloster, S., Lamarque, J.-F.,

360   Liousse, C., Masui, T., Meleux, F., Mieville, A., Ohara, T., Raut, J.-C., Riahi, K.,

361   Schultz, M.G., Smith, S.J., Thompson, A., van Aardenne, J., van der Werff, G.R., and

362   van Vuuren, D.P.: Evolution of anthropogenic and biomass burning emissions of air

363   pollutants at global and regional scales during the 1980 – 2010 period, Clim. Change,

364   109, 163-190, 2011.

Atmospheric
Chemistry
and Physics
Discussions

365

366 Lindberg, S., Bullock, R., Ebinghaus, R., Engstrom, D., Feng, X., Fitzgerald, W.,

367 Pirrone, N., Prestbon, E., and Seigneur, C.: A synthesis of progress and uncertainties

368 in attributing the sources of mercury in deposition, Ambio, 36, 19-32, 2007.

369

370 Meehl, G.A.: The South Asian monsoon and the tropospheric biennial oscillation, J.

371 Climate, 10, 1921-1943, 1997.

372

373 Meehl, G.A., and Arblaster, J.M.: The tropospheric biennial oscillation and Indian

374 monsoon rainfall, Geophys. Res. Lett., 28, 1731-1734, 2001.

375

376 Meehl, G.A., and Arblaster, J.M.: The tropospheric biennial oscillation and Asian-

377 Australian monsoon rainfall, J. Climate, 15, 722-744, 2002.

378

379 Mergler, D., Anderson, H.A., Chan, L.H.N., Mahaffey, K.R., Murray, M., Sakamoto,

380 M., and Stern, A.H.: Methylmercury exposure and health effects in humans: A

381 worldwide concern, Ambio, 36, 3-11, 2007.

382

383 Muntean, M., Janssens-Maenhout, G., Song, S., Selin, N.E., Olivier, J.G.J., Guizzardi,

384 D., Maas, R., Dentener, F.: Trend analysis from 1970 to 2008 and model evaluation of

385 EDGARv4 global gridded anthropogenic mercury emissions, Sci. Total Environ. 494-

386 495, 337-350, 2014.

387

388 Prestbo, E.M., and Gay, D.A.: Wet deposition of mercury in the U.S. and Canada,

389 1996-2005: Results and analysis of the NADP mercury deposition network (MDN),

390 Atmos. Environ. 43, 4223-4233, 2009.

391

392 Rotty, R.M.: Estimates of seasonal variation in fossil fuel CO_2 emission, Tellus B, 39,

393 184–202, 1987.

394

395 Salmi, T., Määttä, A., Anttila, P., Ruoho-Airola, T., Amnell, T.: Detecting trends of

396 annual values of atmospheric pollutants by the Mann-Kendall test and Sen´s slope

397 estimates – the Excel template application Makesens, Finnish Meteorological

398 Institute, Helsinki, Finland, 2002.

Atmospheric
Chemistry
and Physics
Discussions

13

399

400 Scheuhammer, A.M., Meyer, M.W., Sandheinrich, M.B., and Murray, M.W.: Effects

401 of environmental methylmercury on the health of wild birds, mammals, and fish,

402 Ambio, 36, 12-18, 2007.

403

404 Selin, N.E., Jacob, D.J., Yantoska, R.M., Strode, S., Jaeglé, L., and Sunderland, E.M.:

405 Global 3-D land-ocean-atmosphere model for mercury: Present-day versus

406 preindustrial cycles and anthropogenic enrichment factors for deposition, Global

407 Biogeochem. Cycles, 22, GB2011, doi:10.1029/2007GB003040, 2008.

408

409 Selin, N. E.: Global biogeochemical cycling of mercury: A review, Ann. Rev.

410 Environ. Resour., 34, 43–63, doi:10.1146/annurev.environ.051308.084314, 2009.

411

412 Slemr, F., Brunke, E.-G., Labuschagne, C., Ebinghaus, R.: Total gaseous mercury

413 concentrations at the Cape Point GAW station and their seasonality, Geophys. Res.

414 Lett. 35, L11807, doi:10.1029/2008GL033741, 2008.

415

416 Slemr, F., Brunke, E.-G., Ebinghaus, R., Kuss, J.: Worldwide trend of atmospheric

417 mercury since 1995, Atmos. Chem. Phys, 11, 4779-4787, 2011.

418

419 Slemr, F., Brenninkmeijer, C.A.M., Rauthe-Schöch, A., WQeigelt, A., Ebinghaus, R.,

420 Brunke, E.-G., Martin, L., Spain, T.G., and O´Doherty, S.: El Niño – Southern

421 Oscillation influence on tropospheric mercury concentrations, Geophys. Res. Lett.,

422 43, 1766-1771, 2016.

423

424 Soerensen, A.L., Jacob, D.J., Streets, D.G., Witt, M.L.I., Ebinghaus, R., Mason, R.P.,

425 Andersson, M., Sunderland, E.M.: Multi-decadal decline of mercury in the North-

426 Atlantic atmosphere explained by changing subsurface seawater concentrations,

427 Geophys. Res. Lett. 39, L21810, doi:10.1029/2012GL053736, 2012.

428

429 Sprovieri, F., Pirrone, N., Ebinghaus, R., Kock, H., and Dommergue, A.: A review of

430 worldwide atmospheric mercury measurements, Atmos. Chem. Phys., 10, 8245-8265,

431 2010.

432

Atmospheric
Chemistry
and Physics
Discussions

14

433   Sprovieri, F., Pirrone, N., Bencardino, M., D´Amore, F., Carbone, F., Cinnirella, S.,
434   Mannarino, V., Landis, M., Ebinghaus, R., Weigelt, A., Brunke, E.-G., Labuschagne,
435   C., Martin, L., Munthe, J., Wängberg, I., Artaxo, P., Morais, F., Cairns, W., Barbante,
436   C., del Carmen Diéguez, M., Garcia, P.E., Dommergue, A., Angot, H., Magand, O.,
437   Skov, H., Horvat, M., Kotnik, J., Read, K.A., Neves, L.M., Gawlik, B.M., Sena, F.,
438   Mashyanov, M., Obolkin, V.A., Wip. D., Feng, X.B., Zhang, H., Fu, X.,
439   Ramachandran, R., Cossa, D., Knoery, J., Marusczak, N., Nerentorp, N., and
440   Norstrom.C.: Atmospheric mercury concentrations observed at ground-based
441   monitoring sites globally distributed in the framework of the GMOS network, Atmos.
442   Chem. Phys. Discuss., doi:10.5194/acp-2016-466, 2016.
443
444   Temme, C., Planchard, P., Steffen, A., Banic, C., Beauchamp, S., Poissant, L.,
445   Tordon, R., and Wiens, B.: Trend, seasonal and multivariate analysis study of total
446   gaseous mercury data from the Canadian Atmospheric Mercury Measurement
447   Network (CAM-Net), Atmos. Environ., 41, 5423-5441, 2007.
448
449   Toihir, A.M., Venkataraman, S., Mbatha, N., Sangeetha, S.K., Bencherif, H., Brunke,
450   E-G. and Labuschagne, C. (2015). Studies on CO variation and trends over South
451   Africa AUTHORS: and the Indian ocean using TES satellite data. South African
452   Journal of Science; http://www.sajs.co.za Volume 111; Number 9/10 Sep/Oct 2015.
453
454   Van der Werff, G.R., Randerson, J.T., Giglio, L., Collatz, G.J., Kasibhatla, T.S., and
455   Arellano, Jr., A.F.: Interannual variability in global biomass burning emissions from
456   1997 to 2004, Atmos. Chem. Phys., 6, 3423-3441, 2006.
457
458   Weigelt, A., Ebinghaus, R., Manning, A.J., Derwent, R.G., Simmonds, P.G., Spain,
459   T.G., Jennings, S.G., Slemr, F.: Analysis and interpretation of 18 years of mercury
460   observations since 1996 at Mace Head at the Atlantic Ocean coast of Ireland, Atmos.
461   Environ. 100, 85-93, 2015.
462
463   Weiss-Penzias, P.S., Gay, D.A., Brigham, M.E., Parsons, M.T., Gustin, M.S., and ter
464   Schure, A.: Trends in mercury wet deposition and mercury air concentrations across
465   the U.S. and Canada, Sci. Total Environ., 568, 546-556, 2016.
466

Atmospheric
Chemistry
and Physics
Discussions

Open Access

15

467   Zhang, Y., Jacob, D.J., Horowitz, H.M., Chen, L., Amos, H.M., Krabbenhoft, D.P.,

468   Slemr, F., Louis, V.L.St., and Sunderland, E.M.: Observed decrease in atmospheric

469   mercury explained by global decline in anthropogenic emissions, PNAS, 113, 526-

470   531, 2016.

471

472   Zheng, B., and Liang, J.-Y.: Advance in studies of tropospheric biennial oscillation, J.

473   Tropical Meteorol., 11, 1-9, 2005.

474

Atmospheric
Chemistry
and Physics
Discussions

16

475 **Tables**

476

477 Table 1: Sen´s slopes calculated from monthly GEM averages of all and baseline (i.e. ^{222}Rn ≤

478 250 mBq m^{-3}) data for March 2007 – June 2015.

Data	Sen´s slope [ng m^{-3} year^{-1}]	n	Significance [%]	Range at 95% signif. level [ng m^{-3} year^{-1}]
All data	0.0210	99	>99.98	0.0127 – 0.0284
All Baseline	0.0208	97	>99.98	0.0141 – 0.0280
Fall (MAM, all data)	0.0089	27	95.99	-0.0009 – 0.0198
Fall (MAM, baseline)	0.0108	27	98.78	0.0018 – 0.0223
Winter (JJA, all data)	0.0153	25	99.29	0.0025 – 0.0294
Winter (JJA, baseline)	0.0152	25	98.68	0.0020 – 0.0287
Spring (SON, all data)	0.0375	24	99.74	0.0142 – 0.0556
Spring (SON, baseline)	0.0361	24	99.84	0.0160 – 0.0563
Summer (DJF, all data)	0.0287	23	99.87	0.0119 – 0.0440
Summer (DJF, baseline)	0.0269	21	99.79	0.0020 – 0.0287

479

480

481 Table 2: Least square fit of monthly median of all GEM concentrations for September

482 1995 – December 2004.

483

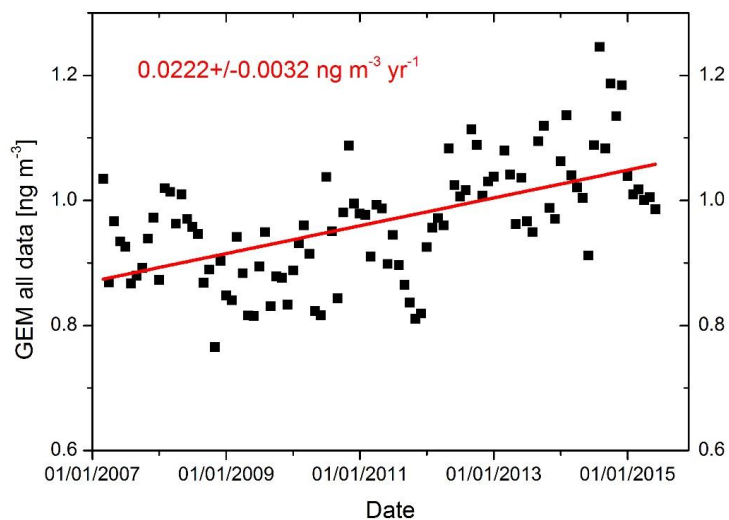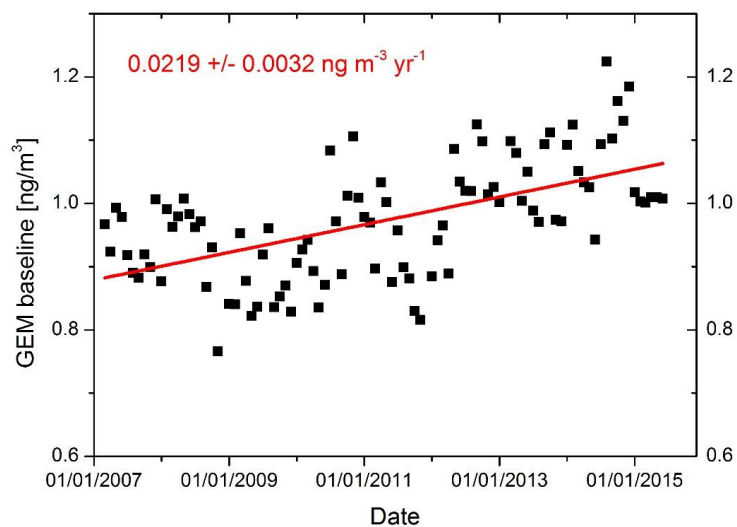| Data	Slope [ng m^{-3} year^{-1}]	n	Signif. level [%]
All data	-0.0176 ± 0.0027	94	>99.9
Fall (MAM)	-0.0132 ± 0.0052	23	>95
Winter (JJA)	-0.0189 ± 0.0049	23	>99.9
Spring (SON)	-0.0198 ± 0.0038	24	>99.9
Summer (DJF)	-0.0154 ± 0.0065	24	>95

484

485

486
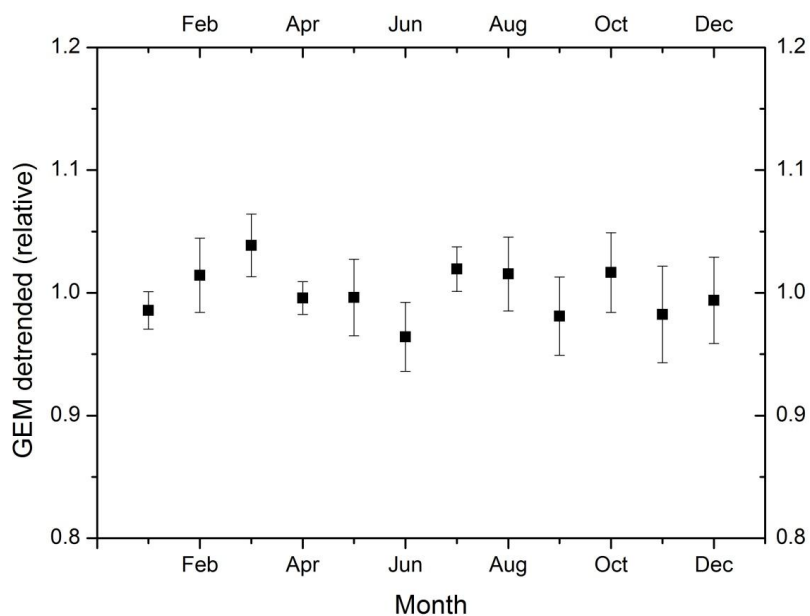
487

17

488   **Figures**

489

490
491   Figure 1: Monthly average GEM concentrations and their least square fit: upper panel

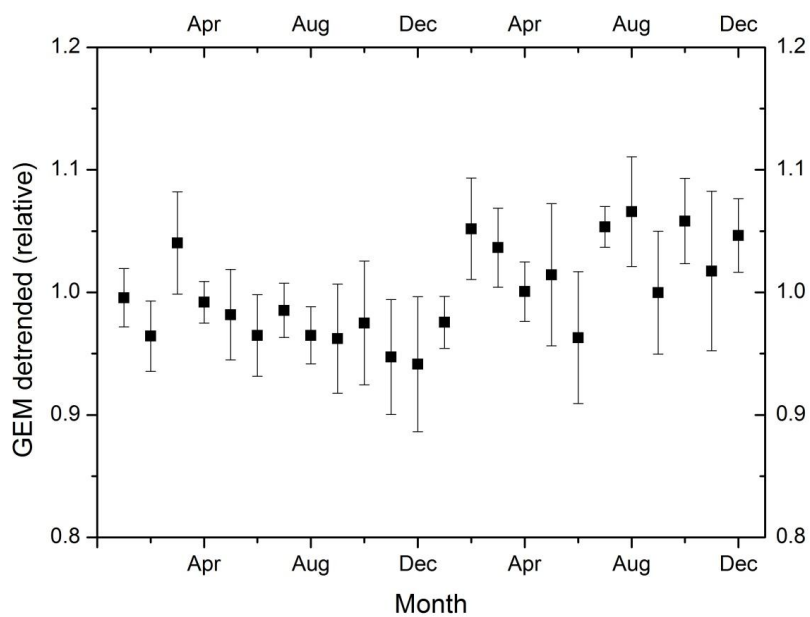492   all data, lower panel baseline data (i.e. only GEM concentrations at ^{222}Rn

493   concentrations ≤ 250 mBq m^{-3}.

494

495

Atmospheric
Chemistry
and Physics
Discussions

Open Access

18

496

497

498   Figure 2: Seasonal (upper panel) and biennial (lower panel) variation of detrended

499   monthly averages. The error bars denote the standard error of the monthly average.